Dalton Transactions

COMMUNICATION

View Article Online
View Journal | View Issue

Cite this: *Dalton Trans.*, 2017, **46**, 3438

Received 16th January 2017,
Accepted 9th February 2017

DOI: 10.1039/c7dt00180k

rsc.li/dalton

Highly efficient cold-white light emission in a $[Au_2CuCl_2(P\cap N)_2]PF_6$ type salt†

Elnaz Hobbollahi,[a] Manuela List,[b] Benjamin Hupp,[c] Fabian Mohr,[d] Raphael J. F. Berger,*[e] Andreas Steffen*[c] and Uwe Monkowius*[a]

In the trinuclear, heterometallic cluster compound $[Au_2CuCl_2(P\cap N)_2]PF_6$ metallophilic interactions give rise to very efficient cold-white light emission as a result of at least two thermally non-equilibrated emissive triplet states (one of mainly Cu → py and the other of Au → py character, respectively) with exceptional spin–orbit coupling and short emission lifetimes, which are competitive to Pt^{II}- and Ir^{III}-based emitters.

The development of emitter materials for opto-electronic applications has accelerated considerably in the last few years. Triplet harvesting has been the dominating concept for emitter materials of organic light emitting devices (OLEDs) since the turn of the millennium.[1] To allow for the harvesting of both singlet and triplet excitons, OLEDs often contain phosphorescent complexes of precious heavy metals such as iridium and platinum.[2] Highly efficient OLEDs can be produced using this technology but also at the cost of some serious drawbacks: rare and thus very expensive metals of yet unclear toxic potential have to be used. In addition, there is an energy loss due to internal conversion from the energy rich singlet to the triplet excited state. However, there are indisputable advantages particular of iridium(III) complexes like high emission quantum yield, tunable emission wavelength, high stability, moderate emission lifetimes in the low μs-time regime and good processability. For example, $[Ir(ppy)_3]$ (ppy = 2-phenylpyridine) and its derivatives can be sublimated (even at high temperatures[3]) without decomposition to produce highly efficient OLEDs with a long device lifetime.

In the last few years, the utilization of thermally activated delayed fluorescence (TADF) emerged as an alternative concept in OELD research. Sometimes also referred to as "singlet harvesting",[4] this approach uses a long known effect of emitting compounds with a small singlet–triplet splitting.[5] In the case that the intersystem-crossing process $S_1 \leftrightarrow T_1$ is sufficiently allowed (intense), the S_1-state can be repopulated from the T_1-state by thermal energy. The occupation of the S_1- and T_1-states is defined by the emission times of both states and the energy difference and can be described by a Boltzmann distribution. A small energetic S_1–T_1 splitting is often found for compounds with a markedly charge transfer character of the excited state. TADF is found in both organic and inorganic compounds. However, to obtain suitable emitter materials with acceptable emission lifetimes in the low μs-time regime, the $S_1 \leftrightarrow T_1$ transition has to be efficient. This is achieved most easily by a heavy atom with an at least moderate high spin–orbit coupling (SOC) constant. Several copper complexes have been suggested as emitter materials as their emission can be assigned to a pronounced metal-to-ligand charge transfer (MLCT) excited state.[5c,6] For some copper phosphane complexes, a TADF was proven or postulated. These complexes show astonishingly high emission quantum yields with emission lifetimes in the order of 10 μs.[6] However, designing TADF emitters is still very challenging as this mechanism cannot be predicted *a priori* and still remains a lucky finding.

In a recent report it was convincingly shown that SOC could be enhanced by additional metal atoms in near proximity to the "emissive" moiety of the molecule.[6k] For example, the presence of a second copper atom in dinuclear copper complexes leads to a significant decrease of the emission lifetimes by still maintaining the high emission quantum yields. The SOC scales roughly with atomic charge Z to fourth order (Z^4), therefore this effect can be increased by adding heavier atoms, *e.g.* 5d transition metals with a closed-shell configurations like gold(I). There have been several publications on Cu–Au heterometallic compounds which are emissive.[7] However, in most of

[a]*Institute of Inorganic Chemistry, Johannes Kepler University Linz, Altenbergerstr. 69, A-4040 Linz, Austria. E-mail: uwe.monkowius@jku.at*
[b]*Institut für Chemische Technologie Organischer Stoffe, Johannes Kepler University Linz, Altenbergerstr. 69, A-4040 Linz, Austria*
[c]*Institut für Anorganische Chemie, Julius-Maximilians-Universität Würzburg, Am Hubland, 97074 Würzburg, Germany. E-mail: andreas.steffen@uni-wuerzburg.de*
[d]*Fakultät für Mathematik und Naturwissenschaften, Anorganische Chemie, Bergische Universität Wuppertal, 42119 Wuppertal, Germany*
[e]*Chemie und Physik der Materialien, Abteilung Materialchemie, Paris-Lodron Universität Salzburg, Hellbrunner Str. 34, 5020 Salzburg, Austria. E-mail: Raphael.Berger@sbg.ac.at*

†Electronic supplementary information (ESI) available. CCDC 1524169 and 1524170. For ESI and crystallographic data in CIF or other electronic format see DOI: 10.1039/c7dt00180k

these studies the photophysical properties were not investigated in detail. In this contribution, we construct a heterometallic trinuclear complex containing formal gold(I) and copper(I) atoms in close proximity bridged by a bidentate P∩N ligand, which surprisingly allows for very efficient cold-white light emission and short emission lifetimes, which are competitive to Pt^{II}- and Ir^{III}-based emitters.

Reaction of the P∩N ligand (P∩N = 2-diphenylphosphano-6-methyl-pyridine) with [AuCl(tht)] (tht = tetrahydrothiophene) leads to the chlorido gold complex [AuCl(P∩N)] (**1**), which after treating with 0.5 equivalent of $[Cu(NCMe)_4]PF_6$ gives the trinuclear cluster $[Au_2CuCl_2(P\cap N)_2]PF_6$ (**2**) in high yields (Fig. 1). All procedures were performed under ambient conditions without further precaution to exclude moisture, and both complexes **1** and **2** are perfectly stable at room temperature under the exclusion of light. The ^{1}H NMR spectra of **1** and **2** show the expected pattern for a coordinated phosphane ligand. The $^{13}P\{^1H\}$ NMR signal of the phosphorus atom shifts from −5.2 ppm for the free ligand to 31.4 ppm for **1** and **2** (Fig. S2†). In the mass spectra, no molecular peaks of the complexes are detected, while the sodium adduct $[\mathbf{1}\cdot Na]^+$ is found at 532.13 (values are given in *m*/*z*); the most intensive signal is found for the cation $[Au(P\cap N)_2]^+$ at 751.31 followed by the signal for $[Au(P\cap N)]^+$ at 474.01. Typical for chlorido gold phosphane complexes,[8] the chloronium ion $[Au_2Cl(P\cap N)_2]^+$ is present as well (983.07). Interestingly, no species containing a copper ion could be detected for **2**. Similar to **1**, the mass spectrum is dominated by ions of $[Au(P\cap N)]^+$ and $[Au_2Cl(P\cap N)_2]^+$.

The identity of **1** and **2** has unambiguously been confirmed by X-ray diffraction using single crystals obtained by gas-phase diffusion of diethyl ether into a solution of the respective complex in dichloromethane (dcm). Although **1** has a lower symmetry compared to $[AuCl(PPh_3)]$, it crystallizes in the same space group $P2_12_12_1$ ($Z = 4$, orthorhombic) with similar metrics.

The gold atom is linearly coordinated by the phosphorus and chlorine atoms with a bond angle of 179.4(1)° for P–Au–Cl and bond length of 2.237(3) and 2.282(3) Å for Au–P and Au–Cl, respectively. The nitrogen atom of the pyridyl moiety points away from the gold atom with a torsion angle of N1–C1–P1–Au1 of 155.2°. The shortest (intermolecular) Au–Au distance is ~6.9 Å, which is well beyond the proclaimed limit of aurophilicity of about 3.5 Å.[9] Interestingly, a related complex of the form [AuCl(P∩N)] with an amyl- instead of a methyl-substituent forms dimers in the crystalline phase showing short 'aurophilic contacts'.[10] Crystals of **2** are triclinic, $P\bar{1}$ with two formula units in the unit cell. The gold atoms are primarily coordinated by phosphorus and the chlorine atoms with a bond angles and lengths very similar to **1**. The copper atom is also coordinated in a linear geometry by the nitrogen atoms of the pyridyl moiety with an N–Cu–N angle of 175.1(1)°. In addition, two gold atoms and one copper atom are forming a triangle stabilized by metallophilic interactions. Considering the van der Waals radii of copper and gold (Cu: 1.40 Å, Au: 1.66 Å),[11] both the distances Au–Au [3.3079(2) Å] and the Au–Cu [2.8087(5) and 2.8374(5) Å] are below the sum of the van der Waals radii of 3.32 Å (Au–Au) and 3.06 Å (Au–Cu, for crystallographic details see Tables S1 & S2†).

In dcm solution, the monogold complex **1** shows absorption maxima at 269 and below 250 nm, and remains non-emissive (Fig. S4†). In contrast, the trinuclear compound **2** features further, but considerably weaker absorption bands at 314 and 366 nm with ε = 2.3 and 7.5 × 10^3 M^{-1} cm^{-1}, respectively, typical for metal-to-ligand charge transfers (MLCT, Fig. 2, 3

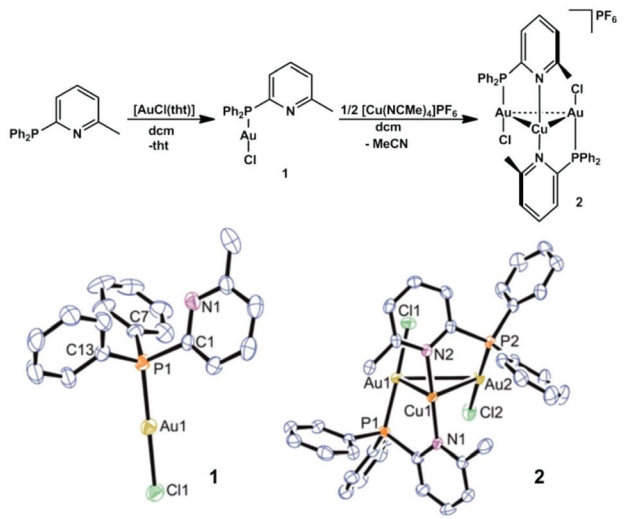

Fig. 1 Top: Synthesis of [AuCl(P∩N)] (**1**) and $[Au_2CuCl_2(P\cap N)_2]PF_6$ (**2**). Bottom: Molecular structures of **1** and the cation of **2** in the solid state determined by single crystal X-ray diffraction. Selected bond lengths [Å] and angles [°]: for **2** Au1–Au2 3.3079(2), Au–Cu 2.887(5)/2.8374(5), Au1–Cu–Au2 71.73(1), Cu–Au–Au 54.54(1)/53.73(1), N1–Cu–N2 175.1(1), P–Au–Cl 177.15(4)/177.47(4).

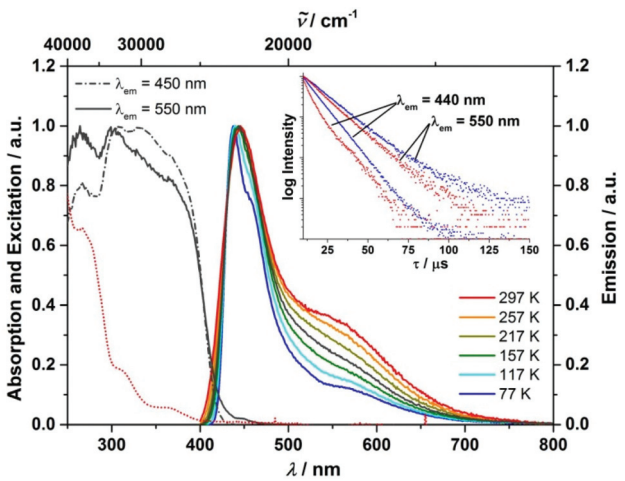

Fig. 2 Absorption spectrum (dotted red) in dcm solution, and temperature-dependent emission (λ_{ex} = 350 nm, solid coloured, normalized to maximum at 450 nm) and -independent excitation (grey) spectra of **2** in the solid state under argon. Inset: Lifetime decays at 297 K (red) and 77 K (blue) recorded at λ_{em} = 440 and 550 nm, respectively. The shape of the decay trace at 297 K/λ_{em} = 440 nm is obscured by the instrument response function, which has no influence on the goodness of fit χ^2 or on the validity of the obtained lifetimes.

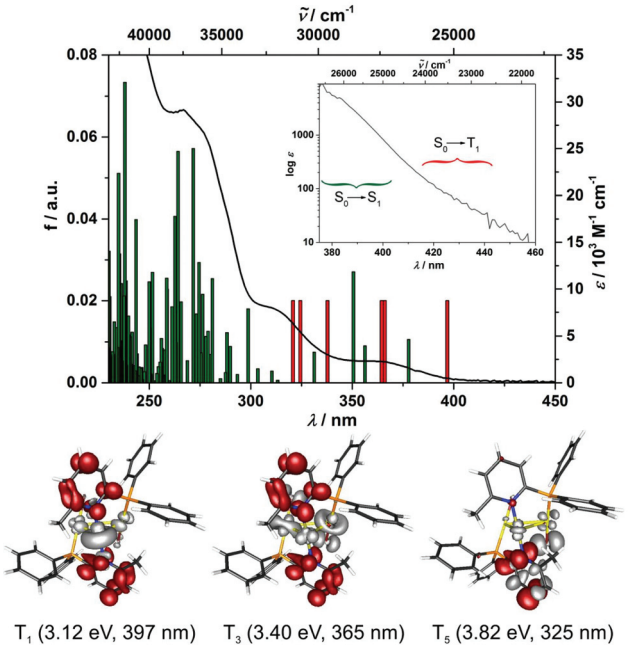

Fig. 3 Top: Experimental absorption spectrum and calculated Franck–Condon (FC) singlet (green) and triplet (red, arbitrary value) transitions at the optimized ground state S_0 geometry of the trinuclear cation of **2** (PBE0/ZORA/def2-TZVP). Bottom: Transition density difference plots and energies of selected $S_0 \rightarrow T_n$ (n = 1, 3, 5) FC transitions.

and S5†). A formally forbidden absorption band is also observed between 410–450 nm (ε = *ca.* 20–80 M^{-1} cm^{-1}), which we assign to the $S_0 \rightarrow T_1$ transition, indicating very strong SOC for d^{10} coinage metal compounds.

Crystalline samples of **2** show dual emission with a sharp high-energy signal at 450 nm and a broad shoulder at *ca.* 550 nm at room temperature (Fig. 2) with an overall quantum yield of φ = 0.28 and CIE 1976 coordinates of u' = 0.40 and v' = 0.89. Thus, **2** is a very efficient cold-white light emitter. The emission is phosphorescence in nature stemming from at least two thermally non-equilibrated triplet states, as indicated by the different lifetimes of $\tau_{450\ nm}$(297 K) = 2.2(77)/6.3(23) μs and $\tau_{550\ nm}$(297 K) = 12 μs (pre-exponential factors are given in brackets). Lowering the temperature to 77 K leads to a larger absolute contribution of the high energy emission band, resulting in nearly pure blue emission with its maximum at 440 nm and a longer lifetime of $\tau_{440\ nm}$(77 K) = 2.1(9)/8.7(91) μs. The low energy band shows only a small change in lifetime to $\tau_{550\ nm}$(77 K) = 13 μs (Fig. 2, inset).

Several implications arise from these findings. Firstly, the participation of TADF, an often found phenomenon for Cu^{I}-based emitters, can be ruled out as this emission mechanism usually leads to an increase in lifetime of 1–3 orders of magnitude and a sigmoidal decay time behavior upon lowering the temperature, which we do not find for the emission between 400–750 nm. Secondly, the low-energy state at λ = 550 nm appears to exhibit *ca.* 90% emission efficiency at 297 K, as lowering the temperature decreases non-radiative decay and increases the observed lifetime. However, the negligible increase in lifetime between 297 and 77 K points to inefficient non-radiative decay at room temperature and an estimated radiative rate constant of $k_r \approx 7.7 \times 10^4$ s^{-1}, which is competitive with Pt^{II}-based emitters, and thus implies strong spin–orbit coupling (SOC) to be present. Thirdly, the increase in lifetime and emission intensity at λ = 450 nm between 297 K and 117 K suggests that non-radiative decay mainly occurs from that triplet state, with the safe assumption of φ_{ISC} = 1.0. However, the negligible changes between 117–77 K suggest 100% emission efficiency at those temperatures, and thus $k_r \approx 1.1 \times 10^5$ s^{-1} due to exceptional strong SOC, which is competitive even with Ir^{III}-based emitters.

To gain more insight into the structure of the electronic states involved in the multiple emissions leading to the observed cold-white light generation and the exceptional short emission lifetimes, we have performed a series of first-principles computations of the trinuclear cation of **2** at the PBE0/ZORA/def2-TZVP level of theory. Geometry optimization yields a structure very similar to the one found in the solid state by single crystal X-ray diffraction (Table S3†). The LUMO and LUMO+1 are π*-type orbitals located at the pyridine ligands, while HOMO to HOMO−5 are dominated by combinations of Cu(d), Au(d) and Cl(p) orbitals (Fig. S6†). Consequently, our TD-DFT calculations, which are in excellent agreement with the experimental absorption spectrum (Fig. 3), show that the low energy bands between λ = 300–400 nm consist of a number of $CuAu_2 \rightarrow$ py CT states with varying Cu and $(AuCl)_2$ participation (Fig. S7†). As a result of the high degree of MLCT involving all three metal atoms, an exceptional SOC for d^{10}-coinage metal compounds is operative and thus explains the experimentally observed $S_0 \rightarrow T_1$ absorption (Fig. 3).

Furthermore, we found that the six energetically lowest triplet transitions are very similar to the respective singlet states in their orbital parentage, thus ensuring strong SOC and high k_r due to the high MLCT degree involving all three metal atoms. The varying contributions from the Cu and $(AuCl)_2$ units in these triplet states should, upon their respective population, result in different changes regarding the metal–metal and Au–Cl bond lengths of the cluster. This presumably allows for geometry relaxations after ISC $S_0 \rightarrow T_n$ into two thermally non-equilibrated emissive excited states.

In order to explore the nature and properties of the triplet states involved in the emission in more detail, including the strength of SOC with the singlet states, we have attempted a SOC calculation of a set of CASSCF-NEVPT2 (as it is implemented in ORCA[12]) states at the equilibrium DFT ground state geometry. Guided by the TD-DFT calculations we constructed the CAS space with a minimal set of active orbitals (localized KS orbitals) by using a d_z^2 type orbital on each Au atom, aligned along the P–Au–Cl bond, and a d_z^2 type orbital on Cu for the occupied orbitals, and the LUMO and LUMO+1, which are of pyridine π*-nature, for the empty active orbitals (CAS 5 and 6). The CAS run was carried out in a state average fashion over 4 singlet and 4 triplet roots. During the CAS-SCF runs it turned out that a symmetric (the cation obeys approxi-

mate C_2 symmetry) combination of the Au-d orbitals is not active in this CAS space, so we have reduced the occupied CAS orbital space to the antisymmetric (*b*) linear combination of the Au-d orbitals and the symmetric (*a*) Cu-d orbital while the unoccupied orbitals were kept (LUMO: py π* (*a*); LUMO+1: py π* (*b*)) yielding an active space [$b^2a^2a^0b^0$]. In this setup the CAS calculation converged. The perturbation correction (NEVPT2) caused a major reordering and significant increase of the energy of the levels ($S_0 \rightarrow S_1$: 357 nm, $f_{osc} = 4.5 \times 10^{-2}$; $S_0 \rightarrow S_2$: 294 nm, $f_{osc} = 6.2 \times 10^{-2}$; $S_0 \rightarrow S_3$: 267 nm, $f_{osc} = 2.7 \times 10^{-2}$) to finally nicely fit the observed absorption spectra (366, 314 and 269 nm). Each of the eight states is mainly constituted from one root and all are in an MLCT relation to the ground state. This also confirms the results of the TD-DFT calculation. Interestingly, S_1 arises from a CT Au → py(π*), while S_2 and S_3 are a result of MLCT Cu(d) → py(π*) which means that this CAS calculation underlines what the TD-DFT calculations already suggested, that there are at least two different non-equilibrating triplet states with Cu → py and Au → py character, respectively from which the observed emission is dominated. The SOC calculation yielded considerable zero-field splitting (*D* constants) of 3.3, 0.7, 0.5 and 10.0 cm^{-1} for the T_1 to T_4 states, respectively, resulting in high oscillator strengths (f_{osc}) for singlet–triplet transitions of 8.2×10^{-5} ($S_0 \rightarrow T_{1z}$, 355 nm, Au → py), 1.4×10^{-4} ($S_0 \rightarrow T_{2x}$, 311 nm, Au → py) and 9.5×10^{-5} ($S_0 \rightarrow T_{3x}$, 295 nm, Cu → py).

The calculated oscillator strengths for the triplet absorptions allow for an approximation of the radiative rate constants k_r of these states by applying the Strickler–Berg equation in the form $k_r = 0.7 \cdot \tilde{\nu}_0^2 \cdot f$, with $\tilde{\nu}_0$ being the energy corresponding to the calculated wavelength of absorption. The values of k_r obtained in this way for T_1, T_2 and T_3 of 4.5×10^4, 1.0×10^5 s^{-1} and 7.6×10^4 s^{-1}, respectively, are in excellent agreement with the experimental values obtained from our temperature-dependent time-resolved luminescence studies of 7.7×10^4 and 1.1×10^5 s^{-1}. Thus, the theoretical studies support the photophysical excited state behavior of $[Au_2CuCl_2(P \cap N)_2]PF_6$ (**2**) postulated above.

In conclusion, we report on the synthesis and structural characterization of the trinuclear, heterometallic cluster compound $[Au_2CuCl_2(P \cap N)_2]PF_6$, of which the metallophilic interactions give rise to very efficient cold-white light emission as a result of thermally non-equilibrated emissive triplet states. Exceptionally high radiative rate constants competitive to Pt^{II}- and Ir^{III}-based emitters have been achieved without TADF due to the fact that all three d^{10} coinage metal atoms are involved in the emissive ^{3}MLCT states, ensuring exceptional strong SOC.

UM thanks Prof. G. Knör and the EU (project M00146, "RERI-uasb") for generous support. AS acknowledges the Deutsche Forschungsgemeinschaft (DFG STE1834/4-1, GRK 2112) and Prof. T. B. Marder for generous support.

Notes and references

1 (*a*) *Physics of Organic Semiconductors*, ed. W. Brütting and C. Adachi, Wiley-VCH, Weinheim, 2012; (*b*) *Highly Efficient OLEDs with Phosphorescent Materials*, ed. H. Yersin, Wiley-VCH, Weinheim, 2008.

2 (*a*) H. Yersin, *Top. Curr. Chem.*, 2004, 1–26; (*b*) C. Adachi, M. A. Baldo, M. E. Thompson and S. R. Forrest, *J. Appl. Phys.*, 2001, **90**, 5048–5051.

3 R. J. F. Berger, H.-G. Stammler, B. Neumann and N. W. Mitzel, *Eur. J. Inorg. Chem.*, 2010, 1613–1617.

4 H. Yersin and U. Monkowius, *International Patents WO* 2010/006681A1, 2008.

5 (*a*) Q. S. Zhang, B. Li, S. P. Huang, H. Nomura, H. Tanaka and C. Adachi, *Nat. Photonics*, 2014, **8**, 326–332; (*b*) S. Igawa, M. Hashimoto, I. Kawata, M. Yashima, M. Hoshino and M. Osawa, *J. Mater. Chem. C*, 2013, **1**, 542–551; (*c*) X. L. Chen, R. M. Yu, Q. K. Zhang, L. J. Zhou, C. Y. Wu, Q. Zhang and C. Z. Lu, *Chem. Mater.*, 2013, **25**, 3910–3920; (*d*) H. Uoyama, K. Goushi, K. Shizu, H. Nomura and C. Adachi, *Nature*, 2012, **492**, 234–238; (*e*) J. C. Deaton, S. C. Switalski, D. Y. Kondakov, R. H. Young, T. D. Pawlik, D. J. Giesen, S. B. Harkins, A. J. M. Miller, S. F. Mickenberg and J. C. Peters, *J. Am. Chem. Soc.*, 2010, **132**, 9499–9508.

6 (*a*) T. Hofbeck, U. Monkowius and H. Yersin, *J. Am. Chem. Soc.*, 2015, **137**, 399–404; (*b*) M. Osawa, *Chem. Commun.*, 2014, **50**, 1801–1803; (*c*) D. M. Zink, M. Bächle, T. Baumann, M. Nieger, M. Kuhn, C. Wang, W. Klopper, U. Monkowius, T. Hofbeck, H. Yersin and S. Bräse, *Inorg. Chem.*, 2013, **52**, 2292–2305; (*d*) M. J. Leitl, F. R. Küchle, H. A. Mayer, L. Wesemann and H. Yersin, *J. Phys. Chem. A*, 2013, **117**, 11823–11836; (*e*) R. Czerwieniec, K. Kowalski and H. Yersin, *Dalton Trans.*, 2013, **42**, 9826–9830; (*f*) C. S. Smith and K. R. Mann, *J. Am. Chem. Soc.*, 2012, **134**, 8786–8789; (*g*) C. Hirtenlehner and U. Monkowius, *Inorg. Chem. Commun.*, 2012, **15**, 109–112; (*h*) H. Yersin, A. F. Rausch, R. Czerwieniec, T. Hofbeck and T. Fischer, *Coord. Chem. Rev.*, 2011, **255**, 2622–2652; (*i*) R. Czerwieniec, J. B. Yu and H. Yersin, *Inorg. Chem.*, 2011, **50**, 8293–8301; (*j*) A. Tsuboyama, K. Kuge, M. Furugori, S. Okada, M. Hoshino and K. Ueno, *Inorg. Chem.*, 2007, **46**, 1992–2001; (*k*) J. Nitsch, F. Lacemon, A. Lorbach, A. Eichhorn, F. Cisnetti and A. Steffen, *Chem. Commun.*, 2016, **52**, 2932–2935.

7 (*a*) T. P. Pell, D. J. D. Wilson, B. W. Skelton, J. L. Dutton and P. J. Barnard, *Inorg. Chem.*, 2016, **55**, 6882–6891; (*b*) M. M. Nenzel, K. Chen and V. J. Catalano, *J. Coord. Chem.*, 2016, **69**, 160–167; (*c*) P. F. Ai, M. Mauro, C. Gourlaouen, S. Carrara, L. De Cola, Y. Tobon, U. Giovanella, C. Botta, A. A. Danopoulos and P. Braunstein, *Inorg. Chem.*, 2016, **55**, 8527–8542; (*d*) K. Chen, M. M. Nenzel, T. M. Brown and V. J. Catalano, *Inorg. Chem.*, 2015, **54**, 6900–6909; (*e*) K. Chen and V. J. Catalano, *Eur. J. Inorg. Chem.*, 2015, 5254–5261; (*f*) C. Jobbagy and A. Deak, *Eur. J. Inorg. Chem.*, 2014, 4434–4449; (*g*) M. J. Calhorda, C. Ceamanos, O. Crespo, M. C. Gimeno, A. Laguna, C. Larraz, P. D. Vaz and M. D. Villacampa, *Inorg. Chem.*, 2010, **49**, 8255–8269; (*h*) E. J. Fernandez, J. M. Lopez-de-Luzuriaga, M. Monge, M. A. Rodriguez, O. Crespo, M. C. Gimeno, A. Laguna and

P. G. Jones, *Chem. – Eur. J.*, 2000, **6**, 636–644; (*i*) M. E. Olmos, A. Schier and H. Schmidbaur, *Z. Naturforsch., B: Chem. Sci.*, 1997, **52**, 203–208; (*j*) S. Bestgen, M. T. Gamer, S. Lebedkin, M. M. Kappes and P. W. Roesky, *Chem. – Eur. J.*, 2015, **21**, 601–614; (*k*) K. Chen, C. E. Strasser, J. C. Schmitt, J. Shearer and V. J. Catalano, *Inorg. Chem.*, 2012, **51**, 1207–1209.

8 (*a*) U. Monkowius, M. Zabel, M. Fleck and H. Yersin, *Z. Naturforsch., B: Chem. Sci.*, 2009, **64**, 1513–1524; (*b*) U. Monkowius, S. Nogai and H. Schmidbaur, *Z. Naturforsch., B: Chem. Sci.*, 2003, **58**, 751–758; (*c*) H. Schmidbaur, A. Hamel, N. W. Mitzel, A. Schier and S. Nogai, *Proc. Natl. Acad. Sci. U. S. A.*, 2002, **99**, 4916–4921.

9 H. Schmidbaur and A. Schier, *Chem. Soc. Rev.*, 2012, **41**, 370–412.

10 E. Tomas-Mendivil, R. Garcia-Alvarez, S. E. Garcia-Garrido, J. Diez, P. Crochet and V. Cadierno, *J. Organomet. Chem.*, 2013, **727**, 1–9.

11 A. Bondi, *J. Phys. Chem.*, 1964, **68**, 441–451.

12 I. Schapiro, K. Sivalingam and F. Neese, *J. Chem. Theory Comput.*, 2013, **9**, 3567–3580.